

Autler-Townes splitting of a cascade system in ultracold cesium Rydberg atoms

Hao Zhang, Limei Wang, Jie Chen, Shanxia Bao, Linjie Zhang, Jianming Zhao,* and Suotang Jia
*State Key Laboratory of Quantum Optics and Quantum Optics Devices, Laser Spectroscopy Laboratory, Shanxi University,
 Taiyuan 030006, People's Republic of China*

(Received 7 November 2012; published 27 March 2013)

Autler-Townes (AT) splitting is observed in ultracold cesium Rydberg gases. Frequency and power of the laser field coupling $6S_{1/2}$ and $6P_{3/2}$ levels are tuned to influence the population redistribution of $6P_{3/2}$ and nS levels excited by another light. The profile of AT spectroscopy is measured experimentally and compared with the theoretical simulation considering the estimated large dephasing rates caused by interaction between Rydberg atoms, which demonstrates that splitting and profile of AT spectra are strongly dependent on the interaction between Rydberg atoms. Rabi frequency of the coupling laser and transition dipole moment of $6S_{1/2} \rightarrow 6P_{3/2}$ are deduced via fitting the measured space variation of two splitting peaks, which is consistent with theoretical calculations.

DOI: [10.1103/PhysRevA.87.033835](https://doi.org/10.1103/PhysRevA.87.033835)

PACS number(s): 42.50.Hz, 32.80.Rm

I. INTRODUCTION

Autler-Townes (AT) splitting [1] and electromagnetic induced transparency (EIT) are typical quantum interference effects [2,3] and have been extensively investigated experimentally and theoretically [4]. In early experiments with thermal atomic vapor, the spectroscopy is strongly affected by the motion of atoms, known to form an obvious Doppler background [5]. A theoretical method has been developed to narrow the linewidth broadening according to this effect [6], and the Doppler-free configuration has also been experimentally realized to investigate the dispersive properties of EIT [7]. An atomic sample could be cooled down to magnitudes of μK or even nK with laser cooling and trapping techniques, which provide an ideal model to investigate interactions between light and matter inducing EIT and AT splitting, etc. [8,9]. These interference effects can be used to study various physical phenomena, such as slow light [10], four-wave mixing [11], enhancement of spin-orbit interaction [12] and dephasing rates of Rydberg states [13].

Rydberg atoms, with principal quantum number $n \gg 1$, possess the exaggerated characteristics compared to ground-state atoms, such as big size, large dipole moment, and strong long-range dipole-dipole interactions, which makes them candidate for quantum gate and information processes [14]. Rydberg atoms also have long lifetimes [15]. Therefore, AT or EIT splitting becomes possible in the cascade three-level system, of which one level is the Rydberg state. Weatherill *et al.* have experimentally investigated EIT in a weakly interacting Rydberg gas [16], nondestructively detected the Rydberg atoms via EIT [17], and furthermore demonstrated a giant electro-optic effect using the polarizable Rydberg dark state [18]. Teo *et al.* [19] have investigated the influence of coupling light on the spectra of AT splitting. Müller *et al.* [20] have proposed a theoretical approach to demonstrate a parallelized CNOT gate based on EIT in the strong and long-ranged interacting Rydberg atoms. Photon-photon interactions can be addressed in the three-level ladder system, including Rydberg states, which are in the strong-interaction regime [21], and

strong dipole-dipole interactions between Rydberg atoms can be mapped onto the optical field [22].

In this work, AT spectra of the ladder three-level system involved Rydberg state are observed in a magneto-optical trap (MOT). The dependences of AT profiles on the detunings and Rabi frequencies of the coupling laser are investigated. Comparing to the former work [19], we especially address the dephasing of the system owing to the strong interaction of Rydberg atoms, which strongly affected the AT spectra and is deduced by fitting the experimental data.

II. EXPERIMENTAL SETUP

We use cesium atoms as experimental samples, which are cooled down to about $100 \mu\text{K}$ with Gaussian radius of about $400 \mu\text{m}$ in a conventional MOT [see Fig. 1(c)]. The details of the setup have been described in our previous work [15]. In this setup, we use three-dimensional trapping lights with 4 mW of power and 8-mm diameter, and we obtain cold atom number and density to be of the order of $\sim 10^7$ and $\sim 10^{10} \text{ cm}^{-3}$, respectively, which is determined by measuring the fluorescence of $6P_{3/2}$ with a calibrated CCD camera (IMC-82FT, IMT Tech.).

We use a two-photon transition scheme to form a cascade three-level system with ground state $6S_{1/2}$ as $|1\rangle$, intermediate state $6P_{3/2}$ as $|2\rangle$, and nS Rydberg state as $|3\rangle$, which is shown in Fig. 1(a). In each experimental cycle, the MOT laser is turned off for $2 \mu\text{s}$ and coupling and probe lasers with durations of $1 \mu\text{s}$ are switched on simultaneously. The coupling light, provided by an extended-cavity diode laser (DL100, Toptica), is first locked to the crossover between $6S_{1/2} F = 4 \rightarrow 6P_{3/2} F' = 4$ and $6S_{1/2} F = 4 \rightarrow 6P_{3/2} F' = 5$, then shifted 90–135 MHz to the transition of $6S_{1/2} F = 4 \rightarrow 6P_{3/2} F' = 5$ by an acoustic-optical modulator (AOM). The first order of the AOM out is collimated to a full width at half maximum (FWHM) of 1 mm. The probe laser, $6P_{3/2} \rightarrow nS$, is accomplished by applying a laser (around 510 nm) measured by a wavelength meter (HighFinesse-Angstrom WSU-30), which is provided by a doubled-frequency laser system (TA-SHG110, Toptica) with linewidth of smaller than 2 MHz. The 510-nm laser is chopped into $1\text{-}\mu\text{s}$ pulses by another AOM, forming a $50\text{-}\mu\text{m}$ radius spot and

*Corresponding author: zhaojm@sxu.edu.cn

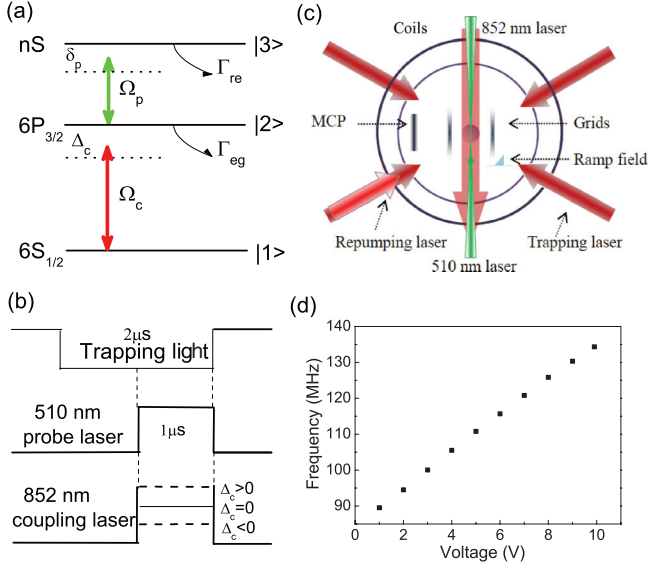


FIG. 1. (Color online) (a) Sketch of the two-photon excitation scheme of cesium. (b) Time sequence of trapping and two excitation lasers. (c) Scheme of MOT and 852- and 510-nm excitation lasers. (d) Frequency shift of the first order vs the modulation voltage of AOM.

counterpropagating through the cold cloud with the coupling laser. In this case, the power of the 852-nm excitation laser that the atoms experience is assumed to be uniformly distributed in the shining volume of the 510-nm laser. After excitation, a ramp field with a rising time of $3\mu s$ and maximum magnitude of 200 V/cm is applied on nonmagnetic grids to ionize Rydberg atoms, and resulted ions are detected by a microchannel plate (MCP) detector. The signals are sampled by a boxcar integrator (SRS250) and recorded with a high-speed DAQ (PCI-1714, Advantech). The main time sequence is controlled by a digital delay or pulse generator (DG535) with a repetition rate of 10 Hz .

The AOM used in the optical path of coupling light is a key device in this experiment. We tune the frequency of the coupling laser red-detuned, resonance, and blue-detuned to the transition of $6S_{1/2} F = 4 \rightarrow 6P_{3/2} F' = 5$ by changing the modulation voltage of the AOM. The variation of the first-order light is compensated so that Rabi frequency of coupling laser Ω_c is constant when we tune the frequency of the coupling laser.

III. EXPERIMENTAL RESULTS AND DISCUSSIONS

Configuration of AT spectroscopy is realized in a cascade system consisting of three levels and two lasers, which is shown in Fig. 1(a). The measured AT spectroscopies with different detunings of the coupling light from $\Delta_c = -2\pi \times 20$ to $+2\pi \times 5\text{ MHz}$ are shown in Fig. 2(a). The power of the 852-nm excitation laser is maintained to be 3 mW throughout the procedure of changing Δ_c . It is clear to observe that the resonant line splits into two peaks, the heights of which are equal at $\Delta_c = 0$. When the coupling light is red-detuned, two peaks of the AT spectroscopy are asymmetric, and the two peaks are almost mirror reflected for the coupling laser red- and blue-detuned. Increasing the detuning of coupling laser

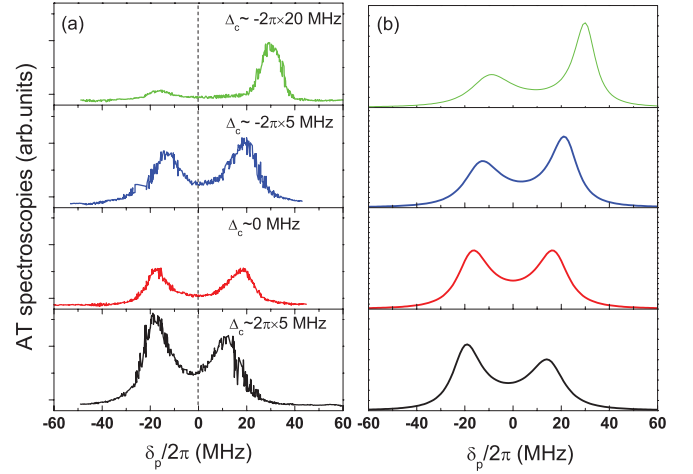


FIG. 2. (Color online) Measurements (a) and calculations (b) of AT spectrum profiles at $\Omega_c = 2\pi \times 36\text{ MHz}$ and different coupling laser detuning Δ_c ranging from $-2\pi \times 20$ to $2\pi \times 5\text{ MHz}$. The up level of the three-level system is the $49S$ state.

Δ_c leads to enlargement of the space between two peaks. Moreover, the space between two peaks varies proportionally with the detuning of the coupling light.

In order to understand the obtained result, we consider a ladder three-level system involving the Rydberg state. The Hamiltonian of the system can be written as

$$H = H_0 + H_{AL}, \quad (1)$$

in which H_0 is the unperturbed Hamiltonian and H_{AL} represents the interaction between light and atoms.

Expanding the Hamiltonian in the space of $|1\rangle$, $|2\rangle$, and $|3\rangle$, and considering the rotating-wave approximation, the Hamiltonian can be expressed in the form of a matrix as

$$H = \begin{pmatrix} 0 & \Omega_c & 0 \\ \Omega_c & -2\Delta_c & \Omega_p \\ 0 & \Omega_p & -2(\Delta_c + \delta_p) \end{pmatrix}, \quad (2)$$

in which Ω_c and Ω_p are Rabi frequencies of the coupling and probing lasers, respectively, and Δ_c and δ_p are the detunings of the coupling and probing lasers, respectively. The Rabi frequency of the transition can be generally expressed as

$$\Omega = \frac{\mu_{ij}}{\hbar} \sqrt{\frac{2P}{\pi\omega^2 c\epsilon_0}}. \quad (3)$$

Here μ_{ij} is the transition dipole moment between two states $|i\rangle$ and $|j\rangle$, P is the power of the laser coupling the transition, and ω is the radius of the laser waist. c and ϵ_0 are the speed of light and permittivity in vacuum, respectively. The Rabi frequency $\Omega_{c(p)}$ is tuned by changing the power of the corresponding laser, whereas condition $\Omega_c \gg \Omega_p$ is always satisfied.

Considering the strong interaction between Rydberg atoms, the system can be described using the motion equation of the density matrix ρ :

$$\dot{\rho} = \frac{i}{\hbar}[H, \rho] + \Gamma, \quad (4)$$

where Γ refers to the dissipation and dephasing of the three-level system, which has intensive influence on the profile of

AT spectra. It can be written in matrix form [13]:

$$\Gamma = \begin{pmatrix} \Gamma_{eg}\rho_{22} & -\frac{1}{2}\gamma_2\rho_{12} & -\frac{1}{2}\gamma_3\rho_{13} \\ -\frac{1}{2}\gamma_2\rho_{21} & -\Gamma_{eg}\rho_{22} + \Gamma_{re}\rho_{33} & -\frac{1}{2}(\gamma_2 + \gamma_3)\rho_{23} \\ -\frac{1}{2}\gamma_3\rho_{31} & -\frac{1}{2}(\gamma_2 + \gamma_3)\rho_{32} & -\Gamma_{re}\rho_{33} \end{pmatrix}. \quad (5)$$

Here Γ is connected to the decay γ_2 and γ_3 of two up levels $|2\rangle$ and $|3\rangle$. $\gamma_2 = \gamma_e + \Gamma_{eg}$ refers to the dephasing of intermediate state $6P_{3/2}$; Γ_{eg} is the spontaneous decay rate of the $6P_{3/2}$ state, which is $2\pi \times 5.2$ MHz [23]; and γ_e is the decay related to the interaction between ground-state atoms, which can be neglected compared to Γ_{eg} . $\gamma_3 = \gamma_r + \Gamma_{re}$ is the dephasing rate of the Rydberg state; here Γ_{re} represents the natural width of the Rydberg state, which is trivial corresponding to the long lifetime of the Rydberg state that is proportional to n^3 [24]. γ_r stems from the strong long-range interactions between Rydberg atoms, which is the dominant contribution to the dephasing of the Rydberg state in the ladder three-level system.

For the steady situation, the imaginary part of ρ_{23} , which is responsible for the absorption of the probe laser represented with ion signals of Rydberg states in this experiment, is expressed as [3]

$$\text{Im}(\rho_{23}) \propto \frac{4(\delta_p + \Delta_c)^2\gamma_2 + \gamma_3(|\Omega_c|^2 + \gamma_2\gamma_3)}{||\Omega_c|^2 - (i\gamma_3 - 2\delta_p)[i\gamma_2 - 2(\delta_p + \Delta_c)]|^2} \quad (6)$$

The calculated profiles of AT spectroscopies with different detunings of the coupling laser are shown in Fig. 2(b). It demonstrates that the profiles of AT spectroscopies are asymmetric at $\Delta_c \neq 0$ and the space between two peaks increases with coupling laser detuning increase, and the simulation is consistent with experiments. By comparing the experimental result and the theoretical calculation, for the 49S state, we obtain that γ_3 is taken to be five times γ_2 , that is, $\gamma_3 = 5\gamma_2$. It is clear to see that the dephasing induced by the strong interaction between Rydberg atoms is much larger than that of the ground state.

Figure 3(a) presents AT spectroscopies with $\Delta_c = 0$ and different Rabi frequencies of coupling laser $\Omega_c = \Omega_0$, $3\Omega_0$, and $4\Omega_0$, where $\Omega_0 = 2\pi \times 15$ MHz together with theoretical simulations in Fig. 3(b). We can see that the distance between two splitting peaks becomes smaller and the signal amplitude goes higher as Ω_c decreases. We obtain the resonant spectrum [see Fig. 3(a), solid curve] at $\Omega_0 = 2\pi \times 15$ MHz instead of two peaks at coupling laser $\Delta_c = 0$. We attribute this phenomenon to the large dephasing owing to the strong long-range interaction between Rydberg states. This long-range interaction has the form of $\sim \frac{C_6}{R^6}$, and $C_6 = 8.12 \times 10^{-60}$ J m⁶ for the 49S state [25]. As mentioned above, we assign this effect as γ_r , which is a component of dephasing γ_3 . γ_r is an important parameter for investigation of the quantum interference and also greatly modifies the long lifetime of the Rydberg state, which makes the interference between two excitations collapse. The decay rate of 49S Rydberg state γ_r can be obtained to be about $2\pi \times 25$ MHz by comparing the calculated Rabi frequency and measured spacing of AT spectroscopy.

As mentioned above, the large decay of the Rydberg state comes from the long-range interaction between Rydberg atoms, which is of the form $\sim \frac{C_6}{R^6}$ and strongly dependent on

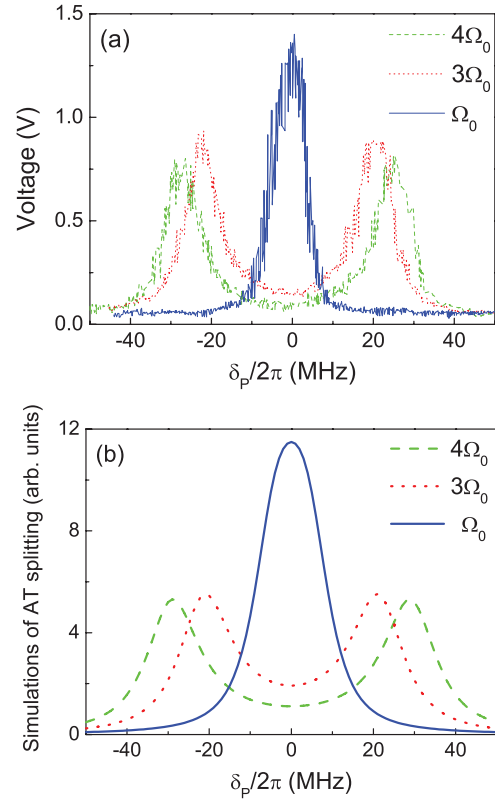


FIG. 3. (Color online) Measured (a) and simulated (b) AT spectra with $\Delta_c = 0$ and different Rabi frequencies of the coupling light of $\Omega_c = \Omega_0$ (blue solid line), $3\Omega_0$ (red dots), and $4\Omega_0$ (green dashed line), where $\Omega_0 = 2\pi \times 15$ MHz and the dephasing rate of Rydberg states is assumed to be $\gamma_3 = 5\gamma_2$. γ_2 represents the dephasing of $6P_{3/2}$.

the density of Rydberg atoms. Here we vary the density of Rydberg atoms by changing the 510-nm laser power with neutral-density filters and further varying the decay rate γ_r . Figure 4(a) presents measured (up panel) and calculated (down panel) AT spectra with Rydberg densities of N_0 and $0.17N_0$ at $\Delta_c = -2\pi \times 5$ MHz and $\Omega_c = 2\pi \times 12$ MHz. The measured dependences of AT splitting on Rabi frequencies of the coupling laser with $\Delta_c = -2\pi \times 5$ MHz and different Rydberg densities of N_0 (blue squares) and $0.17N_0$ (red circles) are also shown in Fig. 4(b). The measured splitting value is obtained by subtracting the central frequencies of two peaks which are fitted with multipeak Lorentz simulation. The large decay not only modifies the profile of AT spectra but also affects the space between two peaks. The dephasing induced with the strong interaction between Rydberg atoms suppresses the quantum interference and leads to the decrease of space and dip between two peaks.

We introduce $\eta = \Omega_c/\gamma_3$ to characterize the behavior of this kind of three-level system. When Ω_c becomes larger or γ_3 smaller, η becomes larger, and the splitting becomes clear. If η becomes small, the quantum coherence properties of the three-level system are destroyed due to strong interaction between atoms, resulting in large dephasing and the splitting disappearing, even the coupling laser resonant with transition.

Figure 5 shows the dependence of splitting on the Rabi frequencies of the coupling laser with $\Delta_c = 0$ (black squares) and $\Delta_c = -2\pi \times 20$ MHz (red circles). When $\Delta_c = 0$, the

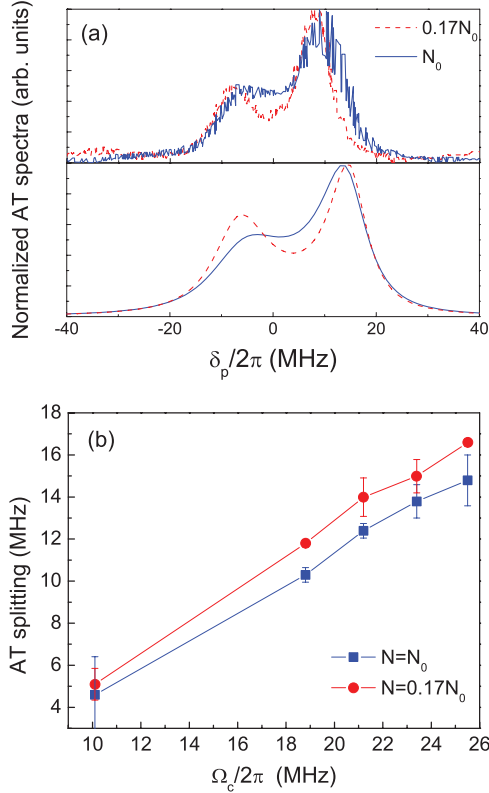


FIG. 4. (Color online) (a) Measurements (up) and simulations (down) of AT profiles with different Rydberg atomic densities N_0 (blue solid line) and $0.17N_0$ (red dashed line). (b) Measured dependences of AT splitting on Rabi frequencies of the coupling laser under different densities of Rydberg atoms N_0 (blue squares) and $0.17N_0$ (red circles) ($\Delta_c = -2\pi \times 5$ MHz).

splittings change linearly with Ω_c while the space enlarges and nonlinearity appears when the coupling laser is detuned to the transition $6S_{1/2} \rightarrow 6P_{3/2}$; similar results were obtained in [19].

We also investigate the dependence of splitting on detunings of the coupling laser. By diagonalizing the Hamiltonian in

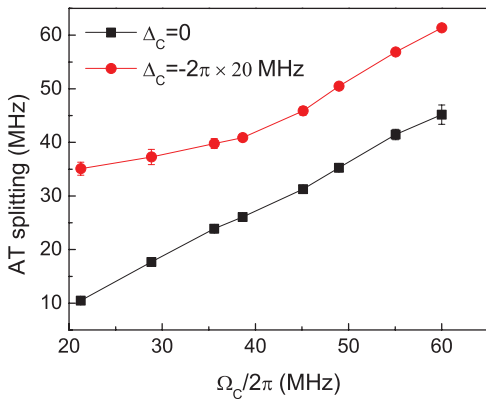


FIG. 5. (Color online) Measured dependence of AT splitting on Rabi frequency of coupling laser Ω_c with different detunings of the coupling laser of $\Delta_c = 0$ (black squares) and $\Delta_c = -2\pi \times 20$ MHz (red circles).

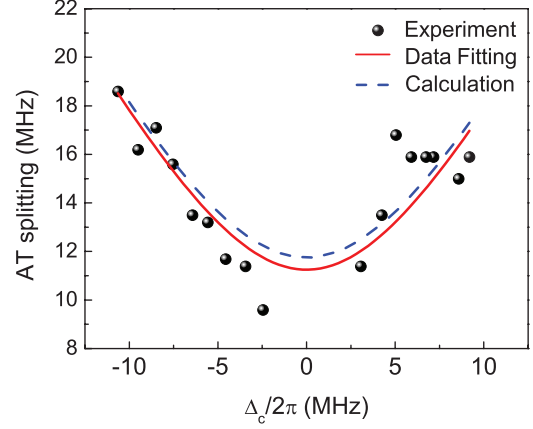


FIG. 6. (Color online) Experimental data (black spheres) with fitting (red solid line) and theoretical calculation (blue dashed line) of splitting spacing between two peaks vs the detunings of the coupling laser. The up level of the three-level system is the $70S$ state.

Eq. (2), we can write the eigenvalues as

$$E \propto \frac{\Delta_c}{2} \pm \sqrt{\left(\frac{\Delta_c}{2}\right)^2 + \left(\frac{\Omega_c}{2}\right)^2} \quad (7)$$

and the splitting between two peaks as

$$\Delta E = \alpha \sqrt{\left(\frac{\Delta_c}{2}\right)^2 + \left(\frac{\Omega_c}{2}\right)^2}, \quad (8)$$

where α is the fitting parameter for consistency of the experimental data and the theoretical calculation. The space between two peaks is dependent on the detuning and the Rabi frequency of the coupling laser. In the experiment, we keep Rabi frequency Ω_c constant and change the detuning Δ_c of the coupling laser by varying the modulation voltage of AOM; the probe laser is tuned to couple the transition of $6P_{3/2} \rightarrow 70S$. The measured spaces of AT splittings are shown in Fig. 6 together with the calculation (dashed line). The large deviation between the experimental measurement and the calculation in the blue-detuned side may come from the variation of coupling laser power owing to large detuning that is far from the central frequency of AOM.

We fit the experimental data using Eq. (8) as shown with the red solid line in Fig. 6 (here $\alpha = 1/2$) and obtain the Rabi frequency of the coupling laser to be $\Omega_c = 51.0 \pm 7.8$ MHz. Using Eq. (3), the transition dipole moment μ_{12} for $|1\rangle$ ($6S_{1/2}$) \rightarrow $|2\rangle$ ($6P_{3/2}$) is also deduced to be about $2.58 \pm 0.40ea_0$, which is close to the calculated value of $\mu_{12} = 2.73ea_0$ [26]. For comparison we list the experimental result and some theoretical calculation values of μ_{12} with [27] and without considering the hyperfine structure of cesium in Table I. The deviation between the measurement and the calculation may be attributed to the dephasing of the system being added

TABLE I. Experiment and calculation of dipole moment for transition $6S_{1/2}$ ($F = 4$) \rightarrow $6P_{3/2}$ ($F' = 5$).

	Expt.	Cal.	Ref. [27]
$\mu_{12}(ea_0)$	2.58 ± 0.40	2.73	3.17

empirically in the equation of density operator [Eq. (4)]. In future work, we will incorporate this strong interaction in the Hamiltonian instead of adding the dephasing term empirically, which should describe the phenomenon more fundamentally.

IV. CONCLUSION

We have observed the asymmetric Autler-Townes splitting spectroscopy in the cascade three-level system involved Rydberg atom. Two long-lived states of the ground state and Rydberg state, together with the transient intermediate state, consist of a typical cascade system for AT spectroscopy. The measured dependences of profiles and distance between AT splittings on the detuning and Rabi frequency of coupling light are in excellent agreement with the theoretical simulation. The AT spectrum also provides a possible method to measure the dipole moment. The dephasing rate γ_3 owing to the interaction among Rydberg atoms was found to be much larger than γ_2 ,

and the strong interaction in the cascade three-level system involved Rydberg atoms plays an important role in quantum effects. A detailed understanding of the dephasing process in a quantum system is essential for coherent controlling over quantum matter. The ultracold Rydberg gases will be used to study the decoherence phenomenon and corresponding theory in the quantum system.

ACKNOWLEDGMENTS

We gratefully acknowledge useful discussions with Professor Mengjia Sun. This work was supported by 973 (Grant No. 2012CB921603), International Science and Technology Cooperation Program of China (Grant No. 2011DFA12490), NSFC Project for Excellent Research Team (Grant No. 61121064), and the National Natural Science Foundation of China (Grants No. 61078001, No. 11274209, No. 10934004, and No. 60978001).

-
- [1] S. H. Autler and C. H. Townes, *Phys. Rev.* **100**, 703 (1955).
 [2] M. O. Scully and M. S. Zubairy, *Quantum Optics* (Cambridge University Press, Cambridge, 1997).
 [3] M. Fleischhauer, A. Imamoglu, and J. P. Marangos, *Rev. Mod. Phys.* **77**, 633 (2005).
 [4] S. E. Harris, J. E. Field, and A. Imamoglu, *Phys. Rev. Lett.* **64**, 1107 (1990).
 [5] M. Sargent, III, M. O. Scully, and W. E. Lamb, Jr., *Laser Physics* (Addison-Wesley, Reading, 1974).
 [6] A. Javan, O. Kocharovskaya, H. Lee, and M. O. Scully, *Phys. Rev. A* **66**, 013805 (2002).
 [7] M. Xiao, Y. Q. Li, S. Z. Jin, and J. Gea-Banacloche, *Phys. Rev. Lett.* **74**, 666 (1995).
 [8] M. Mitsunaga and N. Imoto, *Phys. Rev. A* **59**, 4773 (1999).
 [9] Q. Liang, B. Yang, J. Yang, T. Zhang, and J. Wang, *Chin. Phys. B* **19**, 113207 (2010).
 [10] L. V. Hau, S. E. Harris, Z. Dutton, and C. H. Behroozi, *Nature (London)* **397**, 594 (1999).
 [11] D. A. Braje, V. Balić, S. Goda, G. Y. Yin, and S. E. Harris, *Phys. Rev. Lett.* **93**, 183601 (2004).
 [12] E. H. Ahmed, S. Ingram, T. Kirova, O. Salihoglu, J. Huennekens, J. Qi, Y. Guan, and A. M. Lyyra, *Phys. Rev. Lett.* **107**, 163601 (2011).
 [13] U. Raitzsch, R. Heidemann, H. Weimer, B. Butscher, P. Kollmann, R. Löw, H. P. Büchler, and T. Pfau, *New J. Phys.* **11**, 055014 (2009).
 [14] L. Isenhower, E. Urban, X. L. Zhang, A. T. Gill, T. Henage, T. A. Johnson, T. G. Walker, and M. Saffman, *Phys. Rev. Lett.* **104**, 010503 (2010).
 [15] Z. G. Feng, H. Zhang, J. L. Che, L. J. Zhang, C. Y. Li, J. M. Zhao, and S. T. Jia, *Phys. Rev. A* **83**, 042711 (2011).
 [16] K. J. Weatherill, J. D. Pritchard, R. P. Abel, M. G. Bason, A. K. Mohapatra, and C. S. Adams, *J. Phys. B* **41**, 201002 (2008).
 [17] A. K. Mohapatra, T. R. Jackson, and C. S. Adams, *Phys. Rev. Lett.* **98**, 113003 (2007).
 [18] A. K. Mohapatra, M. G. Bason, B. Butscher, K. J. Weatherill, and C. S. Adams, *Nature Physics* **4**, 890 (2008).
 [19] B. K. Teo, D. Feldbaum, T. Cubel, J. R. Guest, P. R. Berman, and G. Raithel, *Phys. Rev. A* **68**, 053407 (2003).
 [20] M. Müller, I. Lesanovsky, H. Weimer, H. P. Büchler, and P. Zoller, *Phys. Rev. Lett.* **102**, 170502 (2009).
 [21] A. V. Gorshkov, J. Otterbach, M. Fleischhauer, T. Pohl, and M. D. Lukin, *Phys. Rev. Lett.* **107**, 133602 (2011).
 [22] J. D. Pritchard, D. Maxwell, A. Gauguet, K. J. Weatherill, M. P. A. Jones, and C. S. Adams, *Phys. Rev. Lett.* **105**, 193603 (2010).
 [23] L. Young, W. T. Hill, S. J. Sibener, S. D. Price, C. E. Tanner, C. E. Wieman, and S. R. Leone, *Phys. Rev. A* **50**, 2174 (1994).
 [24] T. F. Gallagher, *Rydberg Atom* (Cambridge University Press, Cambridge, 1994).
 [25] K. Singer, J. Stanojevic, M. Weidemüller, and R. Côté, *J. Phys. B* **38**, S295 (2008).
 [26] $\mu_{12} = \frac{\sqrt{2}}{3} R_{6S_{1/2}}^{6P_{3/2}} q$, and we find $R_{6S_{1/2}}^{6P_{3/2}} = 5.76a_0$.
 [27] D. A. Steck, <http://steck.us/alkalidata> (2010).